Antimony and arsenic exhibit contrasting spatial distributions in the sediment and vegetation of a contaminated wetland

Jan Warnken [a], Rohana Ohlsson [b], David T. Welsh [b], Peter R. Teasdale [c, d], Ariella Chelsky [a], William W. Bennett [b, *]

[a] Australian Rivers Institute, Griffith School of Environment, Griffith University, Gold Coast Campus, QLD 4215, Australia
[b] Environmental Futures Research Institute, Griffith School of Environment, Griffith University, Gold Coast Campus, QLD 4215, Australia
[c] Natural and Built Environments Research Centre, School of Natural and Built Environments, University of South Australia, SA 5095, Australia
[d] Future Industries Institute, University of South Australia, SA 5095, Australia

HIGHLIGHTS

- Spatial dispersion of Sb and As from mine tailings studied in a freshwater wetland.
- Sb was less mobile than As under the prevailing reducing conditions.
- Wetland plants accumulated more As than Sb, despite lower sediment concentrations.
- As presents greater environmental risk due to higher mobility.

GRAPHICAL ABSTRACT
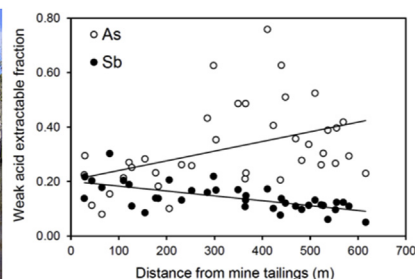
ARTICLE INFO

ABSTRACT

Antimony is a priority environmental contaminant that is relatively poorly studied compared to other trace metal(loid)s. In particular, the behaviour of antimony in wetland sediments, where anaerobic conditions often dominate, has received considerably less attention compared to well-drained terrestrial soil environments. Here we report the results of a spatial assessment of antimony in the sediments and vegetation of a freshwater wetland exposed to stibnite tailings for the past forty years. The concentration of antimony in the sediment decreased rapidly with distance from the tailings deposit, from a maximum of ~22,000 mg kg^{-1} to ~1000 mg kg^{-1} at a distance of ~150 m. In contrast, arsenic was distributed more evenly across the wetland, indicating that it was more mobile under the prevailing hypoxic/anoxic conditions. Less clear trends were observed in the tissues of wetland plants, with the concentrations of antimony in waterlilies (2.5–195 mg kg^{-1}) showing no clear trends with distance from the tailings deposit, and no correlation with sediment concentrations. Sedges and *Melaleuca* sp. trees had lower antimony concentrations (<25 mg kg^{-1} and 5 mg kg^{-1}, respectively) compared to waterlilies, but showed a non-significant trend of higher concentrations closer to the tailings. For all vegetation types sampled, antimony concentrations were consistently lower than arsenic concentrations (Sb:As = 0.27–0.31), despite higher concentrations of antimony in the sediment. Overall, the results of this study highlight clear differences in the behaviour of antimony and arsenic in freshwater wetlands, which should be considered during the management and remediation of such sites.

---

* Corresponding author.
  E-mail address: w.bennett@griffith.edu.au (W.W. Bennett).

1. Introduction

The growing use and demand for antimony (Sb) as flame retardants, lead hardeners and battery or alloy components has pushed annual production to almost 4.2 times the amount of its chemically closest relative, arsenic (As) (U.S. Geological Survey, 2016). The latter has been a priority contaminant for almost a century and its reactions under different environmental conditions are reasonably well understood (Smedley and Kinniburgh, 2002). Knowledge in regard to the reactivity, and therefore mobility and biological uptake, of Sb under different environmental conditions is still developing (e.g. (Tschan et al., 2009; Wilson et al., 2010; Feng et al., 2013; Fu et al., 2016). Existing reviews by Filella et al. (2007), Nakamaru and Altansuvd (2014) and Wilson et al. (2010), and recent work by Fawcett et al. (2015) and Fu et al. (2016) suggest that the mobility of Sb is considerably lower in contaminated soils, even at high concentrations, when compared to As.

Studies investigating Sb dispersion and mobility *in situ* in solid matrices have focused on barren tailing deposits, their surrounding terrestrial soils or stream sediments where samples could be collected using the same methods as for soils (e.g. Okkenhaug et al. (2011); Hiller et al. (2012); Levresse et al. (2012); Fu et al. (2016)). The majority of these matrices were likely to be subject to predominantly oxic conditions and therefore high to moderately high redox potentials.

Sb mobility is known to be influenced by (soil) pore water redox potential (Mitsunobu et al., 2006; Frohne et al., 2011; Hockmann et al., 2014), pH (Leuz et al., 2006b), soil composition and structure (e.g. iron oxides (Leuz et al., 2006a) and Ca (Okkenhaug et al., 2011)), and organic matter content (Steely et al., 2007). Some studies indicate that Sb(III) is less mobile than Sb(V) (Lintschinger et al., 1998; Leuz et al., 2006b). The complexity of the combination and interactions of these factors so far have produced inconclusive results in relation to Sb uptake in higher plants (Feng et al., 2013). In some cases, certain species demonstrated effective exclusion of soil- or pore water Sb, notably in shoots and leaves (e.g. Fu et al. (2016)) while others appear to hyper-accumulate this metalloid in roots and shoots (Feng et al., 2013). A recent investigation of soil contamination with Sb showed a positive, but non-significant trend between soil pH values and Sb bio-accumulation factors (BAFs), indicating low bioavailability under acidic conditions, compared to an inverse trend for As BAFs (and presumably higher bioavailability) in Xikuangshan, China (Fu et al., 2016). These observations, experiments and reviews (Nakamaru and Altansuvd, 2014) suggest that Sb could still be relatively immobile in sediments under anoxic and low pH conditions.

To date, however, few *in situ* investigations have included waterlogged wetland sediments (Nakamaru and Altansuvd, 2014; Fawcett et al., 2015) and to our knowledge no studies have investigated horizontal dispersion in submerged sediments after a major Sb pollution event. In such environments, Sb dispersion will be typically affected by anoxic conditions and low redox potential, as well as high concentrations of humic materials and low pH associated with decomposing plant material. Both, the water column and sediments in such natural wetlands are subject to complex spatio-temporal dynamics (Reddy and DeLaune, 2008) that are difficult to replicate in mesocosm simulations. Oxygen concentrations in these environments, and redox potentials in particular, are affected by diurnal, monthly and seasonal variations in community production and respiration rates, as well as major shifts during heavy rainfalls and floods. Metal(loid) mobility, therefore, is not only the result of a number of physico-chemical and biological processes, but also their time-integrated changes and variations through space. The extent of further impacts of metalloid mobility under such conditions, such as the potential distribution across aquatic and terrestrial food chains, can be initially established from contaminant concentrations in tissues of different types of wetland plants (Cardwell et al., 2002).

This study investigates the two-dimensional spatial distribution of Sb and As in sediments and representative plant species across a semi-enclosed wetland 40 years after a short (4.5 years) but major pollution event associated with the processing of stibnite ore. Tailings were deposited at the inflow section of the wetland, which was located at the end of a small catchment with no other notable sources of Sb. The contaminated site was subsequently closed-off and left undisturbed, without any major rehabilitation works. Under these conditions, the observed Sb and As distributions are considered to be primarily determined by their long-term cumulative biogeochemistry. Detailed examination of these distributions and concentrations of Sb and As in the leaves of waterlilies, sedges and *Melaleuca* sp. trees were used to determine differences in the long-term time-integrated mobility, and risk of persisting contamination, of Sb and As in impacted freshwater wetland sediments under primarily low or stagnant water flow conditions.

2. Materials and methods

2.1. Study site and history

The contamination event that created the conditions investigated in this study occurred in a ~7.5 ha wetland area near the mouth of the Bellinger River in New South Wales, Australia (30°30′20.0″S 153°00′35.9″E). Sb extraction from stibnite ore occurred from 1969 until 1974 on land immediately adjacent to the wetland (Fig. 1). Following separation in a flotation cell, residual tailings were discarded directly onsite without any containment. Aerial photography from 1973 (GHD, 2012) showed tailing deposits occupying an area of ~1 ha, including a section of the main drainage channel. This channel traverses the wetland in a north-east direction and was deepened at some earlier time to establish 'Station Creek', a reserve recorded on the local cadastre. Much of the wetland was cleared for grazing prior to 1969, which showed the creek line on earlier aerial photographs draining eastward across a ledge into a coastal lagoon (Fig. 1). By 1973, the creek line was no longer detectable on black and white aerial photos and much of the site was inundated.

Colour photographs from 1991 showed wetland and vegetation patches very similar to those identifiable on recent high resolution imagery. The wetland is stagnant and depths vary from 0.5 m to 1.0 m in the western (open) section and from 0.5 m to 0 m in the eastern section. The latter was made up of increasingly dense hummocks of sedges and isolated *Melaleuca* sp. trees creating 'islands' and coherent sections above the main water level. A small catchment size (~2.5 km^2), flood lines of a 1:100 flood model and personal observations of water levels after rainfall during field work suggested that water levels and flows were subject to short spikes following local rain events. Mixing with brackish estuarine waters, if any, was restricted to major flood events associated with storm surges and king tides.

The only disturbance of the site occurred in 1980 when a small part of the eastern tailings section and adjoining land were excavated to construct an unfinished L-shaped channel system (Fig. 1). After that event, the site was left fenced off without any notable remediation works.

2.2. Sample collection

This study used a systematic sampling design (SYS, (Wang et al., 2012)). A regular 50 m grid was shifted on top of a rectified aerial photo registered to the local UTM grid (MGA 94 zone 56) using ArcGIS 10.3 to maximise the number of sample sites covering either
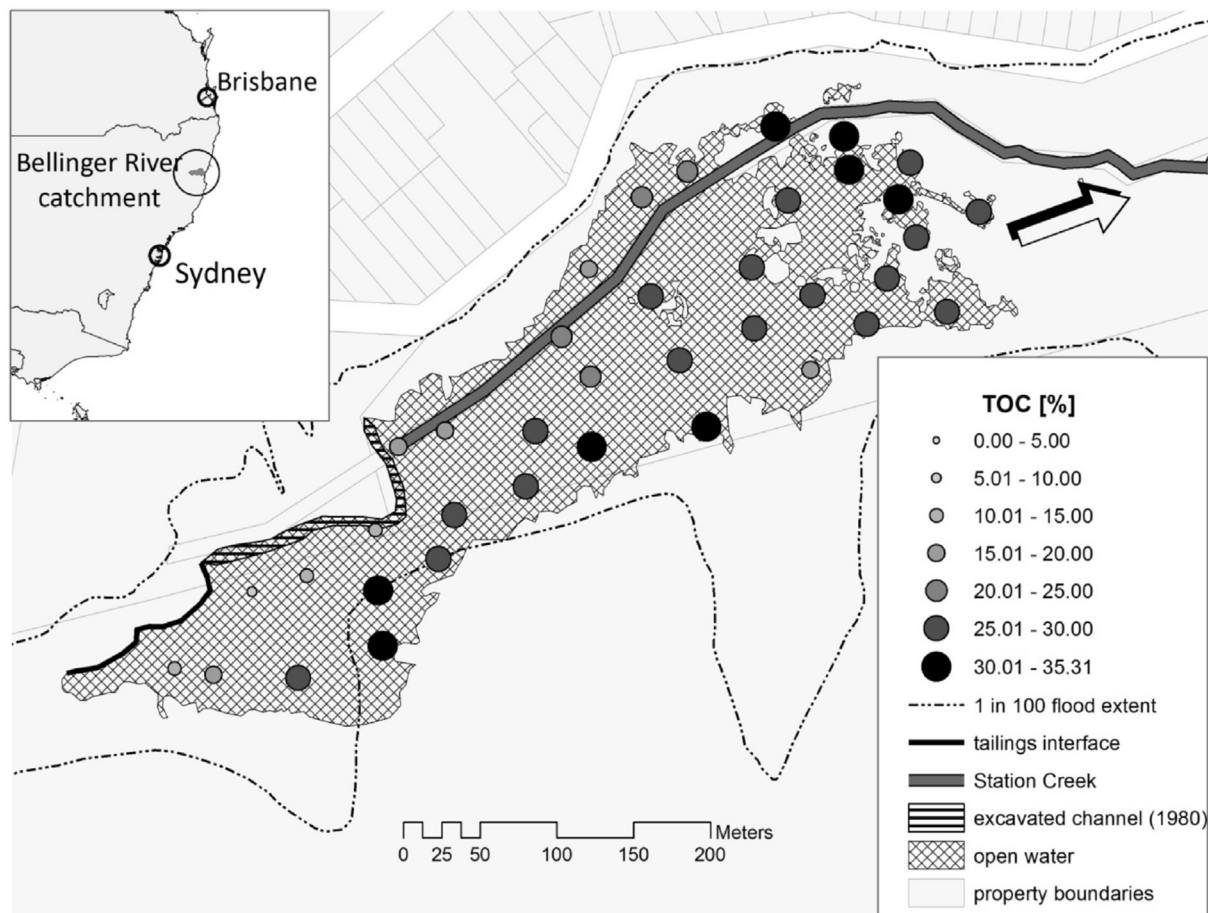
Fig. 1. Study site location, sampling grid layout and total organic carbon (TOC) levels in sediments. Arrows indicate general direction of water flow during high rainfall.

water or wetland vegetation. Sample point coordinates were transferred to a GPS unit (Garmin Oregon 650) and approached by boat or foot. At each location, triplicate sediment samples were collected with an 8 cm-diameter hand corer within an area of approximately 2 m^2. The top 10 cm of each core was transferred to a sealable polyethylene bag and stored the same day at −20 °C for further analysis. The corer was thoroughly washed in site water between samples. Representative samples of leaves (approximately 200 g) from the families *Nymphaeaceae* (waterlilies), *Cyperaceae* (sedges) and *Myrtaceae* (*Melaleuca* sp. trees) were collected from at least three separate plants, where possible, at each sampling location using titanium-coated shears. The distribution of plant species was not consistent, however, so plant material was collected as close as possible to the sediment sampling points.

Water quality parameters including pH, dissolved oxygen, and temperature (°C) were measured *in situ* using a YSI ProPlus multi-parameter instrument calibrated prior to each sampling day. On two separate occasions, oxygen concentrations were measured at 1—5 min intervals over 24—48 h using a HOBO U26 dissolved oxygen logger. The first set of measurements were recorded on the fringes of the wetland in shallow water (<30 cm) in November 2014, and the second set of measurements were recorded in the middle of the ~1 m deep water at the centre of the wetland in June 2015.

2.3. Sample preparation and analysis

Prior to extraction, each sediment sample was thoroughly homogenized for 5 min by hand in an acid rinsed plastic container. Homogenised sediments were split into subsamples for the determination of total acid extractable metal(loid)s (Method 3051A; US EPA (2007)), weak acid extractable metal(loid)s, ratio of dry to wet weight, and total organic carbon content (TOC). TOC was determined for composite sediment samples from each sampling site using a LECO CNS analyser following treatment with HCl to remove carbonates (Skjemstad and Baldock, 2007).

Total extractable metal(loid) concentrations were determined by placing 0.500 g of homogenised wet sediment into a high-pressure perfluoroalkoxy alkane (PFA) microwave vessel with 9.00 mL concentrated ultra-pure (sub-boiling distilled) nitric acid (HNO$_3$) and 3.00 mL concentrated hydrochloric acid (HCl). Following microwave extraction at 175 °C for 10 min in a CEM Mars 6 microwave assisted extraction system, samples were centrifuged for 10 min at 3000 × g. A 200 μL aliquot was diluted 50-fold with deionised water and analysed using Inductively Coupled Plasma − Mass Spectrometry (ICP-MS, Agilent 7900). Calibration standards were prepared in 2% ultra-pure HNO$_3$ from a multi-elemental stock solution (High Purity Standards). A freshwater stream sediment certified reference material (CRM) (NCS DC 73309) was also extracted for every 20 samples and analysed, with typical recoveries of 93—112% for the studied analytes. A quality control standard solution (10 μg L^{-1}) was analysed every 10 samples to monitor for instrument drift.

Weak acid extractable metal(loid) concentrations were determined as described by (Sutherland, 2002). Briefly, 0.500 g of homogenised wet sediment was placed into a 50 mL polypropylene

tube with 10.00 mL of 1 M HCl (Instrument Quality, Seastar). Samples were agitated on a platform shaker for 1 h at 25 °C. After centrifugation for 10 min, a 100 μL aliquot was diluted 50-fold with ultra-pure 2% HNO_3 and analysed by ICP-MS. Dry weight to wet weight ratios were determined by drying a weighed sample of each analysed sediment sample to a constant weight at 105 °C.

Vegetation samples were rinsed in deionised water to remove all adhered foreign material and dried to a constant weight at 60 °C. Waterlily leaves were ground in an agate mortar to create a homogenised sample. Sedge and *Melaleuca* leaf material could not be easily ground, and so were cut into small pieces with titanium-coated scissors and pieces thoroughly mixed to obtain a representative sub-sample. All plant material was digested following US EPA Method 3052 (US EPA, 1996). Briefly, 0.250 g of dried, homogenised sample was weighed into a high-pressure PFA vessel with 9.00 mL concentrated ultra-pure HNO_3, 2.00 mL concentrated HCl and 1.00 mL concentrated H_2O_2 (AR Grade). Samples were digested for 15 min at 180 °C in a CEM Mars 6 microwave assisted extraction system. Following centrifugation (3000 × g, 10 min), a 200 μL aliquot was diluted 50-fold with deionized water and analysed by ICP-MS. The efficiency of the digestion procedure was verified by digesting and analyzing a citrus leaf CRM (NCS ZC 73018), which had typical recoveries of 102–119% for the studied analytes.

Limits of detection (LOD) for the weak acid and total acid extractable metal(loid)s in sediments, and for the plant tissue digestions, were calculated from the standard deviation of procedural blanks taken through the entire extraction and analysis process (Table S1). All sample concentrations were blank corrected.

2.4. Spatial and statistical analyses

The key independent variable, the nearest distance across open water between the tailings deposit and each sampling site, was calculated by digitising the water-land boundary around the main tailings deposit and applying the 'Path Distance' module in ArcGIS 10.3 Spatial Analyst on a 1.5 m raster layer generated from the digitised polygons for open water patches as shown in Fig. 1.

Initial multivariate correlation and regression analyses were calculated using SPSS 22. All data were $\log_{10} (x+1)$ transformed to satisfy the assumption of normality and then tested for spatial autocorrelation (Moran's I) using ArcGIS 10.3 'Spatial Statistics' tool box. Changes in concentrations with distance from tailings deposit were analysed using R's 'segmented' package v 05.-1.4 (Muggeo, 2015), which performs an iterative piecewise regression analysis to identify multiple statistically significant linear regressions in the data set and the point(s) at which they change (i.e. breakpoint(s)). The 'modified *t*-test' module in R's 'SpatialPack' v 0.2−3 (Osorio and Vallejos, 2014), based on Clifford et al. (1989), was used to account for spatial autocorrelation when analysing relationships between Sb and As across the wetland.

3. Results and discussion

3.1. Organic carbon concentrations in wetland sediments

TOC concentrations in sediments (Fig. 1) were higher (25%–35% dry weight) along the southern and eastern sections of the wetland, with lower concentrations (<20%) mostly located along the main drainage line of the wetland. These included those areas that were disturbed either as part of the clearing and drainage prior to the stibnite processing activities, or during and after (i.e. the dumping of tailing spoils and the excavation of the L-shaped channel). The generally high concentration of sediment TOC is consistent with the relatively stagnant nature of this freshwater wetland, which results in accumulation of decaying organic material where

material can be trapped between roots and leaves of nearby sedge tussocks or *Melaleuca* trees and sediment disturbances are on average lowest. In turn, this large quantity of organic matter and the lack of water flow results in depleted oxygen concentrations in the overlying water. Dissolved oxygen concentrations recorded over a diel cycle(s) were often below 25% O_2 saturation and even dropped to 0% at times, even during the day (Fig. S1). The exception to this was in very shallow water (i.e. the edges of the wetland) where oxygen was observed to become saturated in the overlying water during the day (Fig. S2).

3.2. Contaminant concentrations in wetland sediments

The maximum total acid extractable concentration of Sb (22000 mg kg^{-1}) was similar to those previously reported for tailings in Xikuangshan, China (~17000 mg kg^{-1}; Fu et al. (2016)) and Slovakia (~10000 mg kg^{-1}; Hiller et al. (2012)). Observed As maxima were much lower (2500 mg kg^{-1}) and comparable with the highest As levels in soils of Sb mining sites in Slovakia (~1700 mg kg^{-1}; Hiller et al. (2012)) but exceeded maximum concentrations reported for tailings in China (~850 mg kg^{-1}; (Fu et al., 2016)). Minimum total extractable concentrations (150 mg kg^{-1} Sb and 120 mg kg^{-1} As) exceeded those reported by Ashley et al. (2007) (1.1 mg kg^{-1} Sb and 7.9 mg kg^{-1} As) for background concentrations found in stream sediments of the neighbouring Macleay River Basin. The ranges of weak acid extractable concentrations in sediments were lower for both Sb and As, as expected. Maxima and minima for both Sb (3600 mg kg^{-1} to 17 mg kg^{-1}) and As (430 mg kg^{-1} to 62 mg kg^{-1}) were almost an order of magnitude lower than those determined by the total acid extractable procedure. It should be noted that all measured sediment samples exceed the current Australian sediment quality guideline values of 2.0 mg kg^{-1} Sb and 20 mg kg^{-1} As (dry weight) (ANZECC and ARMCANZ, 2000; Simpson and Batley, 2016).

There was greater Sb attenuation with distance from the tailings site compared to As (Fig. 2). Breakpoint analyses further illustrated that the distribution of Sb concentrations were best described when splitting the sample at a single breakpoint, which then explained most of the variation in sediment Sb concentrations based on the distance from the tailings deposit (R^2 values ~ 0.9, Fig. 2). At distances less than the breakpoint, Sb sediment concentrations are likely the result of gradual and diminishing physical settling of processed ore particles with high metal(loid) concentrations. At distances greater than the breakpoint, biogeochemical processes appeared to become more dominant in determining the mobility of Sb. The notably more gradual decrease in As concentrations resulted in the lowest R-squared values for total acid extractable concentrations with distance and no significant regression with distance for weak acid extractable As in sediments (Fig. 2). It should also be noted that the breakpoint regression for total acid extractable As versus distance ($R^2 = 0.524$) was only slightly better at describing the observed relationship than a standard linear regression ($R^2 = 0.408$). The more even distribution of As throughout the wetland, compared to Sb, indicates that As is more mobile than Sb in this system. The identification, or not, of statistically significant breakpoints in the data by the piecewise regression analysis provides an objective way to interpret differences in contaminant dispersion patterns through space.

Comparisons between Sb and As sediment concentrations at all sample sites showed only weak correlations. Excluding sites prior to the breakpoint distances, however, resulted in significant relationships between total and weak acid extractable concentrations of Sb and As (Table 1). Correlations were strongest between Sb_T and Sb_W, and weakest between As_T and As_W. This same subset also revealed the strongest link between Sb_T and As_T with a
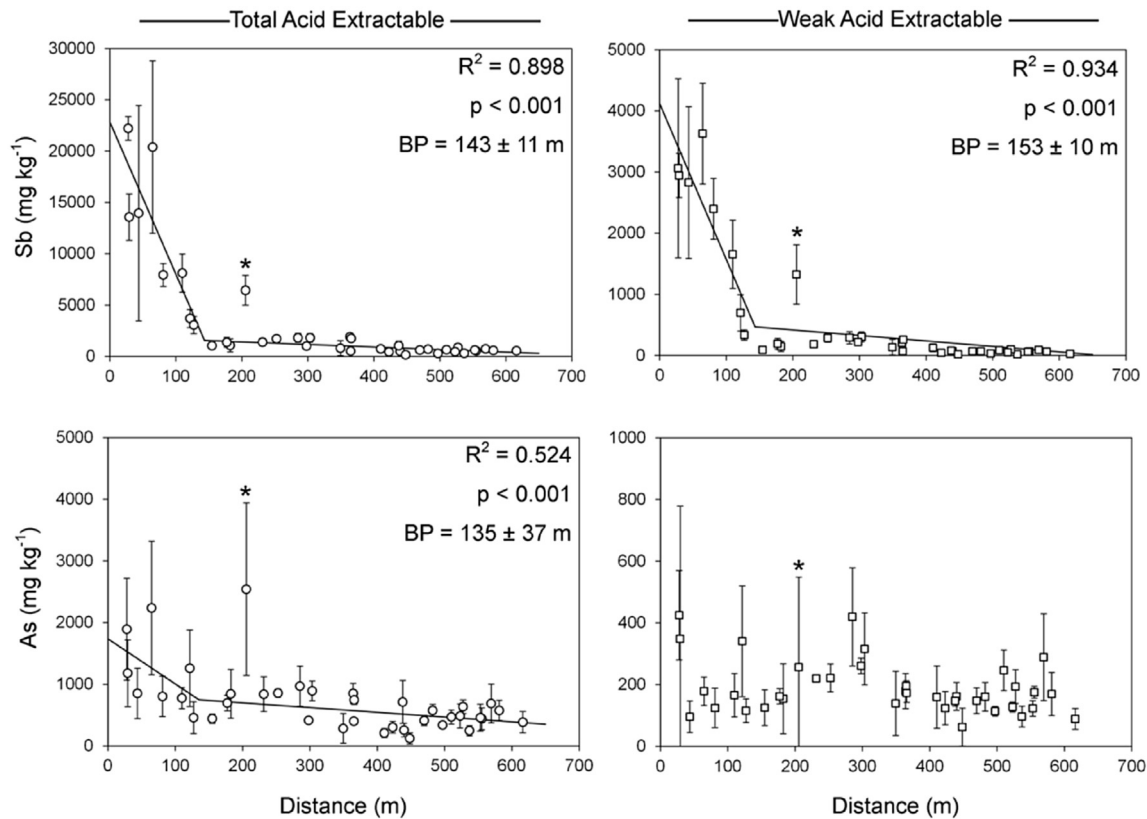
Fig. 2. Total acid extractable (○) and weak acid extractable (□) Sb and As concentrations (mean ± 1 S.D.) for replicate sediment samples (n = 3) against distance from the tailings interface. NOTE: * = point omitted from the regression analysis as an outlier − sediments in this area were disturbed recently and therefore not considered representative of the long-term dispersal of these contaminants.
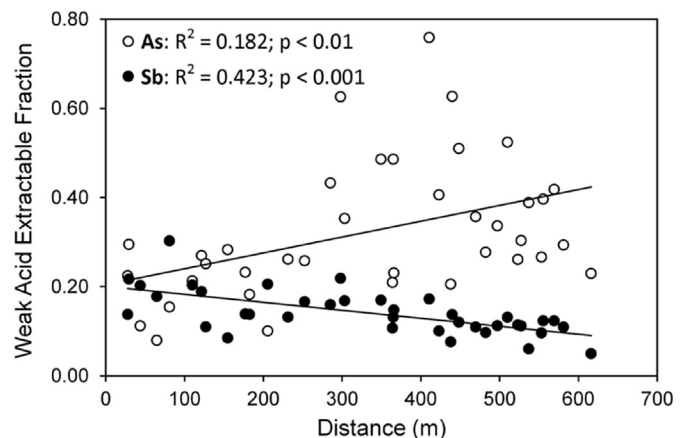
Table 1
Pearson's r and significance (adjusted for spatial autocorrelation) for Sb and As concentrations in wetland sediments (T = total acid extractable concentration; W = weak acid extractable concentration) for samples located after the average breakpoint (138 m). Data were log_{10}-transformed where necessary to meet the assumption of normality.

Variables	n	df	Pearson's r	p
Total vs. weak acid extractable				
$Sb_T − Sb_W$	29	1 + 3.9	0.930	<0.01
$As_T − As_W$	29	1 + 18.3	0.639	<0.01
Sb vs. As				
$Sb_T − As_T$	29	1 + 10.1	0.847	<0.001
$Sb_W − As_W$	29	1 + 9.6	0.703	<0.05

high r^2 value (0.847), low spatial autocorrelation and, therefore, the lowest p-value.

Differences in the distribution of Sb and As in the mostly anaerobic wetland sediments were illustrated by plotting the fraction of weak acid extractable over total acid extractable concentrations against distance from the tailings (Fig. 3). This fraction includes metal(loid)s associated with amorphous, and thus readily-reducible, metal (Fe and Mn) oxyhydroxides and with acid-volatile sulfides, and therefore excludes highly mineralised (and thus less mobile) forms (Sutherland, 2002; Simpson and Batley, 2016). This weak acid extraction is often used to target the potentially bioavailable, and thus more mobile, fraction of metal(loid)s in sediments (Simpson and Batley, 2016). With increasing distance from the stibnite tailings deposit, As_W/As_T and Sb_W/Sb_T fractions showed opposite trends (i.e. a positive and a negative relationship, respectively) (Fig. 3), which indicates that the proportion of potentially mobile As increases with distance, whereas the opposite is the case for Sb.

Fig. 3. Weak acid extractable fraction of the total acid extractable concentration of Sb and As versus distance from the tailings interface. The slopes of the linear regression lines were significantly different (ANCOVA; p < 0.001).

Together the patterns observed in this study suggest that, under the predominantly anoxic conditions that prevail in wetland sediments, the chemical properties of Sb resulted in the element having a considerably greater attenuation over time and therefore, a lower potential for future mobilisation compared to As. Under anaerobic conditions, As(V) is reduced to As(III), shifting the speciation of As towards the less strongly adsorbing and more mobile As(III) species (Bissen and Frimmel, 2003; Oremland and Stolz, 2003; Mitsunobu et al., 2006). Increasing mobility as a result of microbally-mediated

As methylation has also been shown to be more prevalent under low E_H and pH conditions in a controlled experiment using wetland sediment slurries (Frohne et al., 2011). The same authors inferred that methylation of Sb and therefore its mobility would also increase under such conditions, which would support the earlier suggestion by Wilson et al. (2010) concerning Sb mobility in acid sulphate soils. In contrast, Mitsunobu et al. (2006) reported considerably lower mobility of Sb compared to As under low Eh but mildly alkaline conditions in natural settings. Kulp et al. (2013) and Nakamaru and Altansuvd (2014) also expected that Sb would remain geochemically more stable under reducing conditions than under oxidizing conditions due to the lower mobility of Sb(III) (Filella et al., 2002).

Humic materials can also influence Sb distributions by reducing the mobility of Sb(III) in organic-rich soils and sediments due to complexation by a variety of functional groups (e.g. carboxyl, hydroxyl and thiol functional groups) (Buschmann and Sigg, 2004; Wilson et al., 2010). The high concentrations of TOC in the sediments (Fig. 1), the dark brown colour of the water and an amorphous layer of readily resuspended material at the sediment surface, all indicate that high amounts of particulate and dissolved organic matter were present in the studied wetland. Previous research that showed ~30% of Sb(III) being bound to humic acids (Buschmann and Sigg, 2004) compared to only about 10% of total As (Buschmann et al., 2006) could also partly explain lower Sb mobility compared to As at locations past the breakpoint, however, this is an area of Sb geochemistry that is poorly understood and should be the focus of future work.

The role of iron oxyhydroxide minerals in effecting the mobility of As and Sb in the studied wetland is unknown, but given the highly productive nature of the system, and the prevalence of hypoxic/anoxic water-column conditions (Fig. S1 and S2), it is likely that iron(III) oxyhydroxides play a relatively small role. Furthermore, the high concentrations of dissolved organic carbon that are typical in wetlands where there are significant amounts of decaying vegetation, can limit the oxidation of Fe(II) to Fe(III), and thus prevent the formation of appreciable amounts of iron oxyhydroxide minerals, even under relatively oxidising conditions (Theis and Singer, 1974). Further investigation of the dominant mineral phases present in the wetland sediment is necessary to fully explore the role of iron oxyhydroxides in the cycling of arsenic and antimony in this wetland. Additionally, mechanistic studies of As and Sb biogeochemistry in anoxic wetland sediments are required to fully resolve the role of iron in these systems.

In general, the largely anaerobic conditions in the wetland limited the mobility of Sb and, to a much lesser degree, As, compared to that observed in oxidised dry soils (e.g. (Flynn et al., 2003; Diemar et al., 2009). The only major disturbances would have occurred during the mostly heavy rainfall events in this area and possibly even during periods of strong winds. Rain can induce considerable changes in sediment redox and pH conditions in wetlands (Casiot et al., 2007; Frohne et al., 2011) and wind and wind-induced wave action will turn over and mix much of the water column in a shallow wetland such as this (Batzer and Sharitz, 2014). Increased oxygen levels associated with such disturbances could cause biogeochemical changes, and thus changes in the mobilization or sequestration of metal(loid)s. However, it is difficult to separate and consider the individual effects of rain or wind-induced disturbances in more detail, without further mechanistic studies investigating the biogeochemistry of arsenic and antimony in more detail.

The hydrological changes associated with rainfall disturbances could have played an important role. The greater concentrations of TOC along the southern and eastern borders of the wetland (Fig. 1) and generally thicker layers of decomposing plant material

indicated a net transport in a west-east direction. This could have been facilitated by a periodic flow along the main drainage line (Station Creek) after major rain. The prevailing winds could have also contributed to this effect (see Fig. S3 for an annual wind rose). Subsequent return to low-flow and predominantly anaerobic conditions would have reverted the redox and pH conditions to reinstate the considerably greater mobility of As compared to Sb. Accordingly, and under subtropical climate conditions with prolonged periods of low or no rainfall, As in wetland sediments could pose a considerably greater threat as a co-contaminant of Sb mining activities than Sb itself.

3.3. Contaminant concentrations in wetland vegetation

Leaves from *Melaleuca* trees had the lowest concentrations of Sb and As with respective maxima of 4.7 and 9.5 mg kg^{-1}, with concentration generally declining with distance from the tailings deposits (Fig. 4). Sedges revealed a different pattern, with Sb and As concentrations being on average highest at a distance of between 100 and 250 m from the tailings' deposits. At that distance, maximum concentrations reached 19.7 mg kg^{-1} Sb and 44.5 mg kg^{-1} As when excluding one outlier (concentration > 3 S.D. of the means for each metal(loid) at > 250 m). In more distant parts of the wetland, > 300 m from the tailings' deposits, sedges appeared to exclude Sb, with concentrations remaining at levels below the detection limit (Fig. 4, Table 2). Concentrations in waterlilies were the highest of the three plants (Fig. 4), ranging from 2.5 to 195 mg kg^{-1} Sb and 15 to 340 mg kg^{-1} As, without any notable change in relation to distance from tailings (Fig. 4).

There were no significant correlations between Sb or As (both total and weak acid extractable) in sediment and the sampled vegetation. However, there were strong correlations between Sb and As in the leaves of all three plant species (Table 2). Even at locations with extreme Sb concentrations, As in the leaves of all three plants were at least twice as high as those of Sb. Exceptions to this general rule were only found in a few samples with low metal(loid) concentrations close to the method detection limits (i.e. around 1–2 mg kg^{-1} dry weight).

Overall, the observed assimilation of Sb and As by the three types of higher plants investigated in this wetland study was quite similar to what has been reported for other species growing in Sb-contaminated terrestrial soils and water bodies. Water transport and nutrient uptake mechanisms favoured the assimilation of As over that of Sb (Feng et al., 2013), and reversed the ratio of contaminants from on average 3.4:1 (Sb:As) in sediments (Fig. 2) to around 0.3:1 in the plant tissues (Table 2). Under similar conditions, ratios of Sb to As for two samples of *Equisetum* sp. were reported as 0.1:1 and 0.08:1 (Fawcett et al., 2015). There was no evidence of Sb hyper-accumulation (Feng et al., 2011) with the Sb concentrations in the three types of plants in this study never exceeding 50% of even the lowest Sb levels for the mostly terrestrial plants reviewed by Feng et al. (2013).

There was a consistent progression of dry weight metalloid concentrations in the plant leaves of melaleuca < sedges < waterlilies, at all sampling sites where these plants co-occurred (Fig. 4). This order is consistent with their growth forms, as well as their water transport and sources. For submerged stems and leaves of hydrophytes, including waterlilies, water transport is partially direct (i.e. from the water column around stems and leaves to photosynthetically active tissues and from there into the atmosphere during gas exchange). Accordingly, Sb and As present in the water column are likely to provide a major source of contamination in waterlilies (Lavid et al., 2001; Choo et al., 2006). A previous study of the Urunga wetland reported high concentrations of dissolved Sb and As throughout the wetland (up to 155 µg L^{-1} Sb and 118 µg L^{-1}
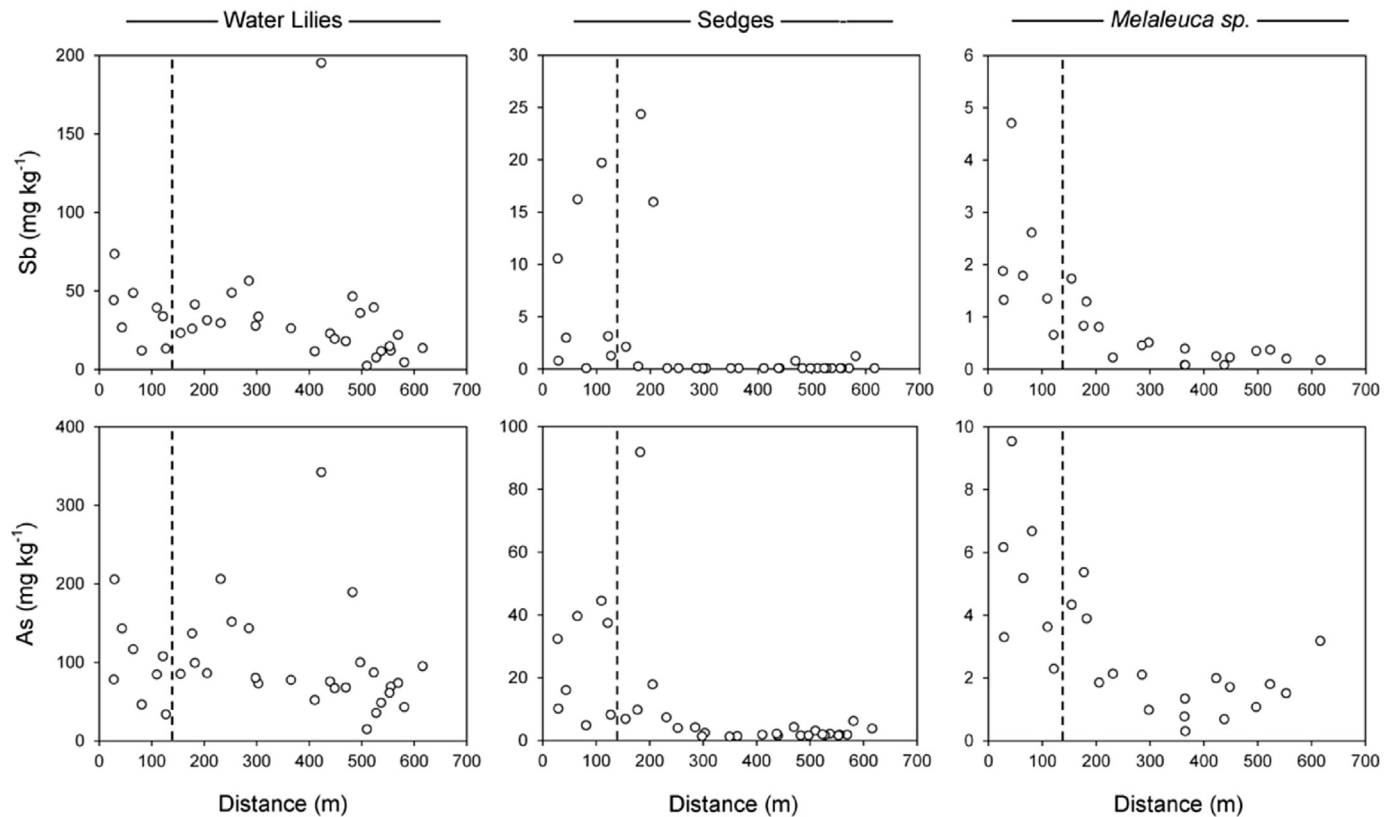
Fig. 4. Tissue concentrations of Sb and As in waterlilies, sedges and *Melaleuca* trees versus distance from the tailings interface. Note the differences in y-axis scales. The dashed line represents the average position of the breakpoint in sediment contaminant concentrations (see Fig. 2).

Table 2
Pearson's correlation analysis results for Sb and As concentrations in wetland plants. The degrees of freedom were adjusted for spatial autocorrelation (SpatialPack in R) where present. Data were log_{10}-transformed where necessary to meet the assumption of normality.

Variables	Ratio ± 1 S.E.	n	df	Pearson's r	p
Melaleuca					
Sb — As	0.27 ± 0.03	24	12.1	0.920	<0.001
Sedges					
Sb — Asˆ	(0.27 ± 0.06)	34 (13)	14.4	0.891 (0.836)	<0.001
Waterlilies					
Sb — As	0.31 ± 0.02	34	21.0	0.862	<0.001

NOTE: n.a. = not applicable; ˆ = 21 samples with Sb concentrations < detection limit where the value of the detection limit was used in the correlation analysis, Pearsons r and ratios calculated without these values shown in italics.

As) (GHD, 2012). Leaf age has also been found to affect the capacity of metal accumulation in waterlilies (Lavid et al., 2001), which could partly explain the high, and spatially independent, variation of Sb and As concentrations observed in these hydrophytes. Overall, the highest concentrations of Sb and As in plant tissues at all sites were found in waterlilies, and no correlations were found between waterlily tissue and sediment concentrations — this is consistent with the water-column being the primary source of Sb and As for uptake by these plants.

In contrast, sedges and *Melaleuca* trees rely on water transport systems typical of terrestrial plants. Almost all water will follow symplastic or, more likely, apoplastic uptake routes across root hair tissues and transport through the xylem to the leaves (Feng et al., 2013). In most plant species, roots have been identified to retain the highest metal(loid) concentrations, which are mostly correlated to concentrations of mobile metal(loid) species in sediment or interstitial pore water (Telford et al., 2009; Fawcett et al., 2015). Sedges take up water via a root system that extends mostly through the upper waterlogged surficial sediment horizon to depths of only 20—30 cm where concentrations are likely to be highest following a contamination incident (Nakamaru and Altansuvd, 2014; Fawcett et al., 2015). In such environments, the sedge investigated in this study may have had an effective mechanism(s) for excluding Sb at low to moderate sediment concentrations (Fig. 4), as has been reported elsewhere for other sedges (*Juncus* spp) (Ashley and Lottermoser, 1999; Craw et al., 2007; Jana et al., 2012). However, at the higher sediment Sb concentrations that occurred before the break point (Fig. 2), metalloid exclusion was not observed, and Sb (as well as As) accumulated in the sedge leaves, albeit to lower concentrations than those observed in waterlilies (Fig. 4).

Sb and As concentrations were lowest in leaves of the slow growing *Melaleuca* trees. Their root systems extend to well below the surficial sediment horizon, beyond the zone where Sb and As concentrations in interstitial pore water were likely to be greatest. This suggests either that transport of Sb and As to these deeper sediments is slow (i.e. via diffusion), or that these trees also have efficient exclusion mechanisms for Sb and As. Metalloid concentrations in *Melaleuca* leaves certainly revealed no major threat to further distribution of Sb and As via herbivorous insects or vertebrates.

4. Conclusions

Results from this study demonstrated that, when left undisturbed, Sb remained geochemically very stable in wetland (i.e. waterlogged) sediments rich in organic matter and covered by a layer of decomposing plant material. Conversely, under these

conditions, As exhibited a more concerning potential for mobility and plant uptake. As is often found in lower but still toxic concentrations in Sb enriched minerals. When processing Sb ores, much of the residual mineral content will be crushed and grated creating tailings particles with large surface areas, which are exposed to processes that facilitate mobilization. Even under the mildly reducing conditions commonly found in freshwater-dominated and predominantly stagnant wetlands, the mobilisation of As over that of Sb appears to be favored. As a result, any remediation work on Sb contaminated soils and sediments should consider the potential mobilisation of associated As. Furthermore, any net increase in soils subject to prolonged waterlogging (e.g. due to climate change and/or sea level rise) could result in spatially more extended transport of As compared to Sb.

Acknowledgements

Appendix A. Supplementary data

Supplementary data related to this article can be found at http://dx.doi.org/10.1016/j.chemosphere.2017.03.142.

References

ANZECC and ARMCANZ, 2000. Australian and New Zealand Guidelines for Fresh and Marine Water Quality. Australian and New Zealand Environment and Conservation Council and Agriculture and Resource Management Council of Australia and New Zealand, Canberra, pp. 1–103.

Ashley, P., Graham, B., Tighe, M., Wolfenden, B., 2007. Antimony and arsenic dispersion in the Macleay River catchment, New South Wales: a study of the environmental geochemical consequences. Aust. J. Earth Sci. 54, 83–103.

Ashley, P., Lottermoser, B., 1999. Arsenic contamination at the mole river mine, northern New South Wales. Aust. J. Earth Sci. 46, 861–874.

Batzer, D.P., Sharitz, R.R. (Eds.), 2014. Ecology of Freshwater and Estuarine Wetlands. University of California Press, Oakland.

Bissen, M., Frimmel, F.H., 2003. Arsenic—a review. Part I: occurrence, toxicity, speciation, mobility. Acta Hydrochim. Hydrobiol. 31, 9–18.

Buschmann, J., Kappeler, A., Lindauer, U., Kistler, D., Berg, M., Sigg, L., 2006. Arsenite and arsenate binding to dissolved humic acids: influence of pH, type of humic acid, and aluminum. Environ. Sci. Technol. 40, 6015–6020.

Buschmann, J., Sigg, L., 2004. Antimony (III) binding to humic substances: influence of pH and type of humic acid. Environ. Sci. Technol. 38, 4535–4541.

Cardwell, A., Hawker, D.W., Greenway, M., 2002. Metal accumulation in aquatic macrophytes from southeast Queensland, Australia. Chemosphere 48, 653–663.

Casiot, C., Ujevic, M., Munoz, M., Seidel, J., Elbaz-Poulichet, F., 2007. Antimony and arsenic mobility in a creek draining an antimony mine abandoned 85 years ago (upper Orb basin, France). Appl. Geochem. 22, 788–798.

Choo, T., Lee, C., Low, K., Hishamuddin, O., 2006. Accumulation of chromium (VI) from aqueous solutions using water lilies (Nymphaea spontanea). Chemosphere 62, 961–967.

Clifford, P., Richardson, S., Hémon, D., 1989. Assessing the significance of the correlation between two spatial processes. Biometrics 123–134.

Craw, D., Rufaut, C., Haffert, L., Paterson, L., 2007. Plant colonization and arsenic uptake on high arsenic mine wastes, New Zealand. Water, Air, Soil Pollut. 179, 351–364.

Diemar, G.A., Filella, M., Leverett, P., Williams, P.A., 2009. Dispersion of antimony from oxidizing ore deposits. Pure Appl. Chem. 81, 1547–1553.

Fawcett, S.E., Jamieson, H.E., Nordstrom, D.K., McCleskey, R.B., 2015. Arsenic and antimony geochemistry of mine wastes, associated waters and sediments at the Giant Mine, Yellowknife, Northwest Territories, Canada. Appl. Geochem. 62, 3–17.

Feng, R., Wei, C., Tu, S., Ding, Y., Wang, R., Guo, J., 2013. The uptake and detoxification of antimony by plants: a review. Environ. Exp. Bot. 96, 28–34.

Feng, R., Wei, C., Tu, S., Tang, S., Wu, F., 2011. Simultaneous hyperaccumulation of arsenic and antimony in Cretan brake fern: evidence of plant uptake and subcellular distributions. Microchem. J. 97, 38–43.

Filella, M., Belzile, N., Chen, Y.-W., 2002. Antimony in the environment: a review focused on natural waters: I. Occurrence. Earth-Science Rev. 57, 125–176.

Filella, M., Belzile, N., Lett, M.-C., 2007. Antimony in the environment: a review focused on natural waters. III. Microbiota relevant interactions. Earth-Science Rev. 80, 195–217.

Flynn, H.C., Meharg, A.A., Bowyer, P.K., Paton, G.I., 2003. Antimony bioavailability in mine soils. Environ. Pollut. 124, 93–100.

Frohne, T., Rinklebe, J., Diaz-Bone, R.A., Du Laing, G., 2011. Controlled variation of redox conditions in a floodplain soil: impact on metal mobilization and bio-methylation of arsenic and antimony. Geoderma 160, 414–424.

Fu, Z., Wu, F., Mo, C., Deng, Q., Meng, W., Giesy, J.P., 2016. Comparison of arsenic and antimony biogeochemical behavior in water, soil and tailings from Xikuang-shan, China. Sci. Total Environ. 539, 97–104.

GHD, 2012. Former antimony processing plant - Urunga NSW detailed investigation report. Coffs Harbour NSW: Crown Lands.

Hiller, E., Lalinská, B., Chovan, M., Jurkovič, Ľ., Klimko, T., Jankulár, M., Hovorič, R., Šottník, P., Fľaková, R., Ženišová, Z., Ondrejková, I., 2012. Arsenic and antimony contamination of waters, stream sediments and soils in the vicinity of abandoned antimony mines in the Western Carpathians, Slovakia. Appl. Geochem. 27, 598–614.

Hockmann, K., Lenz, M., Tandy, S., Nachtegaal, M., Janousch, M., Schulin, R., 2014. Release of antimony from contaminated soil induced by redox changes. J. Hazard. Mater. 275, 215–221.

Jana, U., Chassany, V., Bertrand, G., Castrec-Rouelle, M., Aubry, E., Boudsocq, S., Laffray, D., Repellin, A., 2012. Analysis of arsenic and antimony distribution within plants growing at an old mine site in Ouche (Cantal, France) and identification of species suitable for site revegetation. J. Environ. Manag. 110, 188–193.

Kulp, T.R., Miller, L.G., Braiotta, F., Webb, S.M., Kocar, B.D., Blum, J.S., Oremland, R.S., 2013. Microbiological reduction of Sb (V) in anoxic freshwater sediments. Environ. Sci. Technol. 48, 218–226.

Lavid, N., Barkay, Z., Tel-Or, E., 2001. Accumulation of heavy metals in epidermal glands of the waterlily (Nymphaeaceae). Planta 212, 313–322.

Leuz, A.-K., Hug, S.J., Wehrli, B., Johnson, C.A., 2006a. Iron-mediated oxidation of antimony (III) by oxygen and hydrogen peroxide compared to arsenic (III) oxidation. Environ. Sci. Technol. 40, 2565–2571.

Leuz, A.-K., Mönch, H., Johnson, C.A., 2006b. Sorption of Sb (III) and Sb (V) to goethite: influence on Sb (III) oxidation and mobilization. Environ. Sci. Technol. 40, 7277–7282.

Levresse, G., Lopez, G., Tritlla, J., López, E.C., Chavez, A.C., Salvador, E.M., Soler, A., Corbella, M., Sandoval, L.H., Corona-Esquivel, R., 2012. Phytoavailability of antimony and heavy metals in arid regions: the case of the Wadley Sb district (San Luis, Potosí, Mexico). Sci. Total Environ. 427, 115–125.

Lintschinger, J., Michalke, B., Schulte-Hostede, S., Schramel, P., 1998. Studies on speciation of antimony in soil contaminated by industrial activity. Int. J. Environ. Anal. Chem. 72, 11–25.

Mitsunobu, S., Harada, T., Takahashi, Y., 2006. Comparison of antimony behavior with that of arsenic under various soil redox conditions. Environ. Sci. Technol. 40, 7270–7276.

Muggeo, V.M., 2015. Package 'segmented'. Biometrika 58, 525–534.

Nakamaru, Y.M., Altansuvd, J., 2014. Speciation and bioavailability of selenium and antimony in non-flooded and wetland soils: a review. Chemosphere 111, 366–371.

Okkenhaug, G., Zhu, Y.-G., Luo, L., Lei, M., Li, X., Mulder, J., 2011. Distribution, speciation and availability of antimony (Sb) in soils and terrestrial plants from an active Sb mining area. Environ. Pollut. 159, 2427–2434.

Oremland, R.S., Stolz, J.F., 2003. The ecology of arsenic. Science 300, 939–944.

Osorio, F., Vallejos, R., 2014. SpatialPack: Package for Analysis of Spatial Data. R Package Version 0.2-3.

Reddy, K.R., DeLaune, R.D., 2008. Biogeochemistry of Wetlands: Science and Applications. CRC press - Taylor & Francis, Boca Raton, Florida.

Simpson, S.L., Batley, G.E. (Eds.), 2016. Sediment Quality Assessment: a Practical Guide. CSIRO Publishing, Clayton South, Australia.

Skjemstad, J., Baldock, J.A., 2007. Total and organic carbon (Chapter 21). In: Carter, M.R., Gregorich, E.G. (Eds.), Soil Sampling and Methods of Analysis CRC Press - Taylor and Francis, pp. 225–237. Boca Raton, Florida.

Smedley, P., Kinniburgh, D., 2002. A review of the source, behaviour and distribution of arsenic in natural waters. Appl. Geochem. 17, 517–568.

Steely, S., Amarasiriwardena, D., Xing, B., 2007. An investigation of inorganic antimony species and antimony associated with soil humic acid molar mass fractions in contaminated soils. Environ. Pollut. 148, 590–598.

Sutherland, R.A., 2002. Comparison between non-residual Al, Co, Cu, Fe, Mn, Ni, Pb and Zn released by a three-step sequential extraction procedure and a dilute hydrochloric acid leach for soil and road deposited sediment. Appl. Geochem 17, 353–365.

Telford, K., Maher, W., Krikowa, F., Foster, S., Ellwood, M.J., Ashley, P.M., Lockwood, P.V., Wilson, S.C., 2009. Bioaccumulation of antimony and arsenic in a highly contaminated stream adjacent to the Hillgrove Mine, NSW, Australia. Environ. Chem. 6, 133–143.

Theis, T.L., Singer, P.C., 1974. Complexation of iron(II) by organic matter and its effect on iron(II) oxygenation. Environ. Sci. Technol. 8, 569–573.

Tschan, M., Robinson, B.H., Schulin, R., 2009. Antimony in the soil–plant system—a review. Environ. Chem. 6, 106–115.

U.S. Geological Survey, 2016. Mineral Commodity Summaries 2016. U.S. Geological Survey. http://dx.doi.org/10.3133/70140094.

US EPA, 1996. Method 3052: Microwave Assisted Acid Digestion of Siliceous and Organically Based Matrices (Washington DC).

US EPA, 2007. Method 3051A: Microwave Assisted Acid Digestion of Sediments, Sludges, Soils, and Oils (Washington DC).

Wang, J.-F., Stein, A., Gao, B.-B., Ge, Y., 2012. A review of spatial sampling. Spat. Stat. 2, 1–14.

Wilson, S.C., Lockwood, P.V., Ashley, P.M., Tighe, M., 2010. The chemistry and behaviour of antimony in the soil environment with comparisons to arsenic: a critical review. Environ. Pollut. 158, 1169–1181.